

Signaling Overhead and Power Consumption during Handover in LTE

M. Tayyab
Huawei Technologies Finland Oy
Helsinki, Finland
muhammad.tayyab5@huawei.com

G. P. Koudouridis and X. Gelabert
Huawei Technologies Sweden AB,
Kista, Sweden
george.koudouridis@huawei.com,
xavier.gelabert@huawei.com

R. Jantti
Electrical Engineering Department
Aalto University, Espoo, Finland
riku.jantti@aalto.fi

Abstract— In this paper, we address the signaling overhead and the power consumption that results from the transmission of handover-related signaling in a Long Term Evolution (LTE) cellular network. Specifically, we analyze the contribution of the different signaling messages over the air-interface, and their impact on power consumption both at the eNB and at the User Equipment (UE) during handover (HO). A quantitative analysis is provided using system level simulations. We observe that, within the HO process, the largest contributor to air-interface signaling overhead is the transmission of the measurement report by the UE. This uplink (UL) transmission suffers from different channel impairments, due to interference and transmission range, for particular cell sizes. As a consequence, uplink signaling retransmissions are triggered causing higher signaling load and consequently higher power consumption, this being especially detrimental to battery-powered devices.

Keywords—LTE, handover, signaling overheads, power consumption, performance evaluation, simulation.

I. INTRODUCTION

A key approach to the development of future cellular networks is the cell ultra-densification to satisfy increasing data traffic demands. The spectral efficiency of the network is known to be improved by shrinking the footprints of eNBs, thus reducing the number of users served by each eNB and consequently improving the frequency reuse. In addition to supporting data-hungry applications, cellular networks will need to provide their services to users on the move, probably at increased speeds, within vehicles, or to unmanned autonomous vehicles. One of the limiting factors in densification planning is the HO rate. The gain in capacity achieved by densification is counter-balanced by increased HO rates, since the signaling overhead during the HO procedure interrupts the data flow and thus reduces the user throughput [1]. Densification may also result in high power consumption in both the network and the user device due to frequent HOs, unnecessary HOs with *ping-pong* effects and HO failures (HOF). For the user device in particular, this causes a more detrimental effect on the device battery lifetime. In addition, if a user experiences multiple HOs, the cumulative HO delay will result in a severe deterioration of the perceived user experience [2].

With the above in mind, in this work we will study the signaling overhead and the average supply power consumption that results from the transmission of HO-related signaling over the air-interface in an LTE cellular network. A breakdown of the different signaling transmission contributions will be provided, studying the impact of user speed as well as cell densification and HO parameter selection. In this paper we are specifically interested in the HO

signaling rate over the air-interface, and the related power consumption, in order to identify which parts of the HO procedure are more power consuming.

In related works, an LTE traffic analysis for the signaling load and the energy consumption trade-off in mobile networks was addressed in [3] to obtain the RRC inactivity timer value to save UE's energy at the cost of low increase of the signaling traffic overhead. Noteworthy, a large amount of eNB power consumption models exist in the literature, whereas fewer works are devoted to handset consumption models. A simplified method to calculate the eNB power consumption by considering its main power consuming elements was proposed in [4]. An LTE smartphone overall power consumption model was proposed in [5] including power consumption in idle, connected and discontinuous reception (DRX) mode. In [6], we addressed the impact of cell size and user speed on the HO procedure in an LTE network. We found that both decreasing and increasing ISD, after a certain limit, reveal HO performance degradation. To the best of our knowledge, the study of air-interface signaling and power consumption of the HO procedure has been largely overlooked in the literature. The results obtained herein for the signaling cost and the power consumption during HO are in line with our previous work [6].

The rest of the paper is organized as follows: Section II provides a short overview of the HO mechanism in LTE. Section III discusses the simulator modelling aspects. In Section IV, numerical results and discussion are presented. And finally, Section V provides some concluding remarks.

II. OVERVIEW OF HANDOVER MECHANISM IN LTE

An overall view of the HO procedure in LTE network is shown in Fig. 1 [7]. The procedure is divided into 3 phases: HO preparation, HO execution and HO completion phase. Upon measuring and identifying a better neighboring cell, UE reports to the serving eNB and access the target cell on reception of HO command (from serving eNB). The UE performs signal strength measurements over a specific reference signal received power (RSRP) from the serving cell as well as the neighboring cells. After processing the measurements, if an entry condition is fulfilled, a measurement report (MeasReport) is transmitted to the serving cell. A3 event is used as entry condition to see if the RSRP of the target cell is better than that of the serving cell plus a hysteresis margin (called A3 offset). The entry condition has to be maintained during a time defined by the TTT timer. Once the MeasReport is correctly received at the serving cell, the HO preparation phase between target and serving cell starts and a HO request is transmitted to the t-eNB. Upon successful admission, a HO command (HOcmd) is transmitted from the serving cell to the UE. Upon successful reception of the HOcmd, the HO execution phase starts in which the UE accesses the target cell, by means of a Random

This project has received funding from the European Union's H2020 research and innovation program under grant agreement H2020-MCSA-ITN- 2016-SECRET 722424 [11].

Access Channel (RACH) transmission, and transmits a HO confirmation (HOconf) message. Finally, the t-eNB transmits a HO complete message to the s-eNB to inform the success of HO when the DL path is switched toward the t-eNB. After that the s-eNB releases the allocated resources. In order to achieve a good compromise between HO reliability and HO frequency, HO optimization deals with the adjustment of the TTT and A3 offset [8].

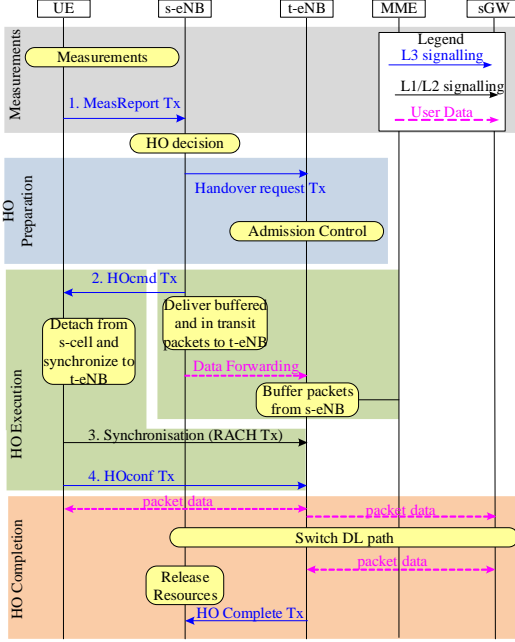


Fig. 1. Intra MME/SG HO Procedure (adapted from [7]).

III. SYSTEM MODEL

A system level LTE simulator is used considering a hexagonal grid of 16 tri-sector eNBs. Cell wrap-around feature is included in order to ensure fair interference conditions across the scenario. A set of 200 UEs is randomly placed over the scenario and the UEs move at a fixed speed in straight lines with random directions $[0^\circ, 360^\circ]$.

As for traffic loading, UEs with UL full-buffer traffic are assumed, thus contributing to UL interference towards other UEs. DL interference is artificially generated by setting the transmission power on a number of randomly selected Physical Resource Blocks (PRBs) given a specific load level (in our case a fully loaded case is assumed).

The simulator implements the main features of the Packet Data Convergence Protocol (PDCP), Radio Link Control (RLC), Medium Access Control (MAC) and physical (PHY) layers including, inter alia, segmentation, Automatic Repeat Request (ARQ) at RLC level, and MAC scheduling with chase combined Hybrid-ARQ (HARQ). For the PHY layer, look-up tables are used which map bit error rate (BER) values to measured subcarrier Signal-to-Interference-and-noise-ratio (SINR) values (via the EESM, Effective Exponential SNR Mapping) in order to account for errors over the wireless link.

The HO model considers the modeling of L3 RRC signaling over the radio access, including measurement reports, handover command and handover confirmation. L2 signaling (UL and DL allocation) is also captured by modeling the PDCCH. Both L2 and L3 signaling are subject to channel impairments and thus prone to RLC failures. Moreover, RLFs

are also considered in the simulator. The main simulation assumptions are summarized in Table I.

Table I Simulation parameters and assumptions.

Feature	Implementation
Network topology	A hexagonal grid of $16 \times 3 = 48$ cells (wrap-around included)
Inter-site distance	From the set $\{125, 250, 500, 1000, 1250\}$ m
System Bandwidth	$B_{sys} = 5$ MHz (paired FDD), with $N_{RB}^{DL} = N_{RB}^{UL} = 25$ RBs at carrier frequency $f_c = 2.6$ GHz
eNB DL power	$P_{eNB} = 43$ dBm
UE Power	$P_{UE} = 23$ dBm
Antenna patterns	3D model specified in [15], Table A.2.1.1.2-2
Channel model	6 tap model, Typical Urban (TU)
Shadowing	Log-normal Shadowing Mean 0 dB, Standard deviation: 8dB
Propagation model	$L = 130.5 + 37.6 \log_{10}(R)$, R in km
UE speed	from the set $\{3, 30, 60, 120\}$ km/h
RLF detection by L1 of UE	T310=1s, N310=1, N311=1 as specified in [16] $Q_{in} = -4.8$ dB; $Q_{out} = -7.2$ dB as specified in [17]
HO parameters	TTT= $\{32, 64, 128\}$ ms, A3 offset = $\{1, 3, 5\}$ dB, L3 filter coefficient $K=4$ (fixed).

A. Power Consumption Model

In the eNB, the radio equipment can be largely divided into the Base-Band Unit (BBU) and the Remote Radio Unit (RRU). In this work, we will focus on the RRU power consumption model, leaving the BBU modelling for future work. Similarly, for the UE, we will only consider the contribution towards power consumption from the RF part. A generic illustration of the eNB and UE components included in the power model is shown in Fig. 2, where $P_{x,sup}$ denotes the necessary supply power to produce an output (transmitted) power P_x , see e.g. [9], where $x = \{eNB, UE\}$. A linear correspondence between $P_{x,sup}$ and P_x is usually assumed in the literature [10]. In this work, we are interested in the contribution of the HO mechanism towards supply power $P_{x,sup}$.

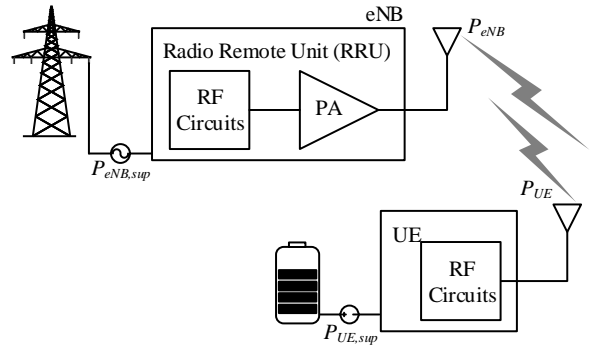


Fig. 2. A simplified overview of the eNB and UE components included in the power model.

In particular, we focus on the HO signaling over the radio interface (Uu) in both UL (UE) and DL (eNB) transmissions, namely: the MeasReport, the RACH and the HOconf transmission from UE and the HOcmd transmission from eNB side (refer to Fig. 1). In order to derive the power consumption of the above signaling transmissions, we proceed by deriving the size of such messages, then the amount of frequency resources needed to transmit these messages, and next the output transmitted power allocated to these resources.

Finally, time duration of these messages or duty cycle is used to compute the time averaged supply power consumption.

The signaling message sizes (in bits) for the MeasReport, HOcmd and HOconf transmissions are denoted as L_s , with subindex $s = \{MR, HOcmd, HOcnf\}$ accordingly.

In LTE, a resource block (RB) is the smallest time-frequency unit being allocated to a user. For a subcarrier spacing of $\Delta f = 15$ kHz, a RB has a bandwidth of $B_{RB} = 180$ KHz (i.e. $N_{sc}^{RB} = 12$ subcarriers) and a time duration of one slot, $T_{RB} = T_{slot} = 0.5$ ms [13]. Alternatively, the RB (or slot) duration can be expressed in terms of the number of symbols it contains, $N_{ymb}^{RB} = 7$, times the symbol length T_{ymb} . A resource element (RE) is then defined as the smallest resource unit consisting of one symbol and one subcarrier to which a modulated symbol is mapped onto. According to the available modulation schemes in LTE, the number of carried bits in a single RE is $L_{RE} \in \{2, 4, 6\}$ bits for QPSK, 16-QAM and 64-QAM modulation respectively. Hence, we can easily derive the number of carried bits per RB, L_{RB} , as

$$L_{RB} = L_{RE} \cdot N_{sc}^{RB} \cdot N_{ymb}^{RB} \cdot \quad (1)$$

It is worthwhile noting that because HOs occur mostly at the cell edge, where the RSRP is low, this justifies our selection of QPSK as the modulation scheme used for the transmission of signalling messages (see Table II for details).

With the above in mind the required number of RBs for each signaling message s , N_{RB}^s , can be obtained by:

$$N_{RB}^s = \left\lceil \frac{L_{RB}}{L_s} \right\rceil, \text{ with } s = \{MR, HOcmd, HOcnf\}, \quad (2)$$

where $\lceil x \rceil$ denotes the smallest integer larger than or equal to x , and, hence it is assumed herein that a signaling message requires an integer number of RBs. In addition, for the RACHtx signaling message, since it carries an un-modulated preamble sequence, we can directly refer to the standard specifications which provides us directly with the value of N_{RB}^{RA} [13] (see Table II).

The power allocation algorithm in both the eNB and the UE will adjust the power level assigned to each subcarrier (and therefore RB) according to the maximum available powers in the eNB (P_{eNB}) and in the UE (P_{UE}) (see Table I). For the case of an equal power allocation algorithm, the allocated power per RB at the eNB and UE can be formulated as:

$$P_{eNB}^{RB} = P_{eNB} / N_{RB}^{DL}, \text{ and} \quad (3)$$

$$P_{UE}^{RB} = P_{UE} / N_{RB}^{UL}, \quad (4)$$

where N_{RB}^{DL} (N_{RB}^{UL}) is the total number of RBs in the DL (UL) given a system bandwidth B_{sys} (see Table I).

It is now straightforward to formulate the allocated transmitted power (in W) per signaling message s as:

$$P_x^s = P_x^{RB} \cdot N_{RB}^s, \text{ and} \quad (5)$$

where $x = \{eNB, UE\}$ and, accordingly, the appropriate number of DL or UL signaling messages should be reflected in N_{RB}^s .

We now may apply some well-known power consumption models for both the eNB and UE, [4][5], in order to obtain the supply power necessary to produce the required transmitted power for each of the signaling messages. In particular, the

supply power for the eNB transmitting signaling s , $P_{eNB, sup}^s$, can be written as

$$P_{eNB, sup}^s = P_{eNB}^s / \eta + P_{RF, eNB} \cdot N_{RB}^s / N_{RB}^{DL}, \quad (6)$$

where P_{eNB}^s is the output transmitted power given by (5) and η accounts for the power amplifier efficiency. $P_{RF, eNB}$ denotes the supply power contribution of the RF equipment, which is conveniently scaled by the portion of utilized resources by signaling message s .

Equally, the supply power required for the UE to transmit signaling message s , $P_{UE, sup}^s$, is given by

$$P_{UE, sup}^s = P_{UE}^s + P_{RF, UE} \cdot N_{RB}^s / N_{RB}^{UL}, \quad (7)$$

where, P_{UE}^s is the output transmitted power given by (5), and where the supply power contribution to the RF part is also scaled by the portion of utilized resources by signaling s .

In order to capture the time-domain system dynamics during transmission and possible retransmissions of signaling messages over the air interface, we define the time-averaged supply power as

$$\bar{P}_{x, sup}^s = P_{x, sup}^s \cdot (\Delta t_x^s / \Delta T), \quad (8)$$

where $P_{x, sup}^s$ ($x = \{eNB, UE\}$) is the ‘‘peak’’ supply power defined in (6)-(7), and $(\Delta t_x^s / \Delta T)$ expresses the duty cycle, or percentage of time where the signalling is actually transmitted. Assuming that the signalling s has a duration of T_x^s seconds (refer to Table II for details) and that a number of N_s signalling messages are transmitted over a period of ΔT seconds, we have that $\Delta t_x^s = T_x^s \cdot N_s$. Finally, we are able to rewrite (8) as:

$$\bar{P}_{x, sup}^s = P_{x, sup}^s \cdot T_x^s \cdot (N_s / \Delta T) = P_{x, sup}^s \cdot T_x^s \cdot R_x^s, \quad (9)$$

where we have defined $R_x^s \triangleq (N_s / \Delta T)$ as the signalling rate which will be obtained from system level simulations. Table II contains the main numerical parameters used in the simulations.

Table II Power Consumption parameters and values.

Feature	Values
Signaling message sizes	$L_{MR} = 128$ bits; $L_{HOcmd} = 296$ bits; $L_{HOcnf} = 96$ bits (according to [14])
Carried bits in a RB	$L_{RB} = 168$ bits (with QPSK modulation, $L_{RE} = 2$)
Number of RBs per each signaling message	$N_{RB}^{MR} = 1$ RB; $N_{RB}^{HOcnf} = 1$ RB; $N_{RB}^{HOcmd} = 2$ RB; $N_{RB}^{RA} = 6$ RB.
Power Amplifier efficiency	$\eta = 0.311$ (31.1%) [4]
RF supply power	$P_{RF, eNB} = 12.9$ W [4] and $P_{RF, UE} = 2.35$ W [5]
Signaling transmission times	$T_{eNB}^{HOcmd} = 0.5$ ms; $T_{UE}^{MR} = 0.5$ ms; $T_{UE}^{HOcnf} = 0.5$ ms; $T_{UE}^{RACHtx} = 1$ ms (we use preamble format 0 according to the cell radius used in simulations, as noted in [12]);

IV. NUMERICAL RESULTS AND DISCUSSION

In this section, we provide a numerical evaluation of the HO procedure in terms of both signaling and power costs.

A. Handover signalling rate analysis

This section shows the numerical results for the signaling rate during HO procedure. Four different types of signaling messages over the radio interface are considered including, measurement report, HO command, RACH and HO confirm

transmission. Simulations are performed according to the models presented in Sec. III, and the results are analyzed for various UE speeds, cell sizes, A3 offset and TTT values mentioned in Table I.

The impact of inter site distance (ISD) and UE speed on an aggregate signaling rate (i.e. the sum of all considered signaling rate transmissions) is shown in Fig. 3. One trend of the graph shows that increasing UE speed, increases the signaling rate which is expected. More interestingly, rising the UE speed contributes to an increase of signaling rate mostly for lower ISDs (125m and 250m). This is because higher UE speeds for small cells will cause moving away from the source cell which may lead to problems during HO and thus increase the signaling overhead. Also, very low ISD (i.e. 125m) suffer from sever interference in the UL since UEs are more likely to be closer to each other and thus experience a high signaling rate owing to successive signaling retransmissions.

The distribution (in %) of the different analyzed signaling messages is shown in Fig. 4. This distribution was obtained averaging over a number of different simulated cases using different input parameters. It is clear from the graph that the highest signaling messages produced are from the MeasReport transmission (38%). This is because the UL transmission suffers from different channel impairments, due to interference and transmission range, for particular cell sizes. As a consequence, MeasReport retransmissions are often triggered which produces performance degradation in terms of increased signaling rate.

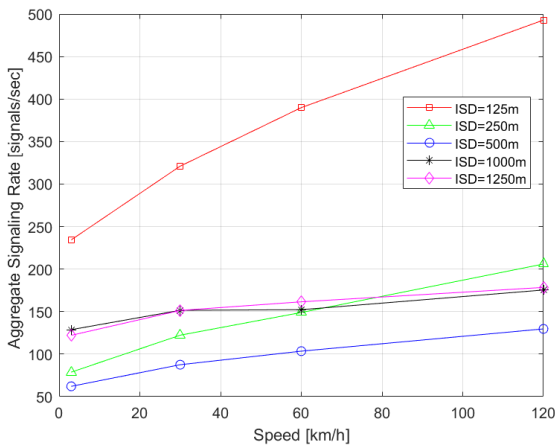


Fig. 3. Impact of ISD and UE speed on the aggregate signaling rate.

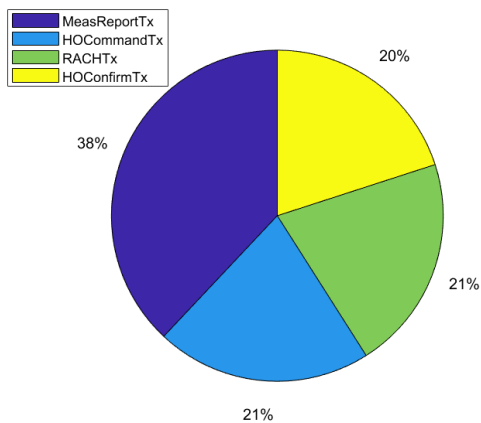


Fig. 4. Average distribution of signalling rate per type.

Fig. 5 shows the impact of A3 offset values on the aggregate signaling rate at fixed speed and TTT. Increasing the offset, decreases the signaling rate, however this comes at the cost of increased HO failures as also noted in [6]. If we compare the trend of offset values for various ISDs, we observe that the aggregate signaling rate is large for low ISDs then it decreases and after that it increases again for high ISDs. As a result of small cell deployment, a higher cell border crossing rate and increased UL interference produce a severe degradation in terms of increased signaling overheads. For large cells (ISD larger than 1000m), UL transmissions at the cell border are damaged due to poor SINR. Fig. 6 shows the impact of TTT values on aggregate signaling rate with signaling breakdown per signaling type at constant speed and offset values. Noting that both the adjustment of the A3 offset and TTT value have similar effects, a similar behavior is observed by varying the TTT between Fig. 6 and Fig. 5.

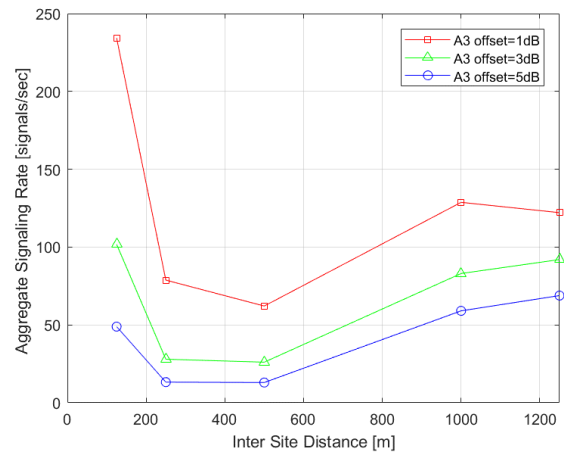


Fig. 5. Impact of A3 offset values on aggregate signaling rate at speed=3 km/h and TTT=32 ms.

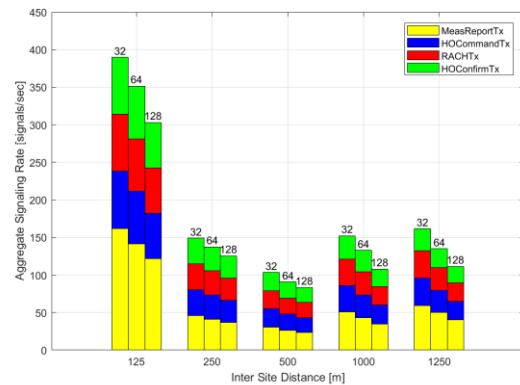


Fig. 6. Impact of TTT values {32, 64, 128} ms on aggregate signaling rate with signaling breakdown per type at speed=60 km/h and offset=1 dB.

B. Power consumption analysis during handover

This section provides the numerical evaluation of the average supply power consumption caused by the different HO signalling transmissions. Fig. 7 shows the impact of ISD on the average supply power consumption of the UE and eNB respectively, as given by (9), at constant speed, offset and TTT values. The power consumption of HO command transmission (DL/eNB power consumption) is much higher as compared to others (UL/UE power consumption). It is clear

from the both graphs that the lowest ISD have the highest power consumption then it decreases and after that it starts increasing again for high ISDs because of the UL impairments as also noted in Fig. 5 and Fig. 6. The lowest power consumption is attained for ISD 500m, which constitutes an “optimum” ISD under the simulated assumptions herein, since we are able to avoid the UL impairment problems arising for small and large ISDs, see also [6].

Fig. 8 shows the per-type signalling power consumption breakdown for the UE. Noteworthy, despite the signalling rate for the MeasReport is higher than for the RACH tx (recall from Fig. 4), because RACH tx takes more RBs, the power consumption is higher in this case. Similar to the signaling rate case, we found that increasing offset and TTT, reduces significantly the power consumption but at the cost of increased HOFs as noted in [6].

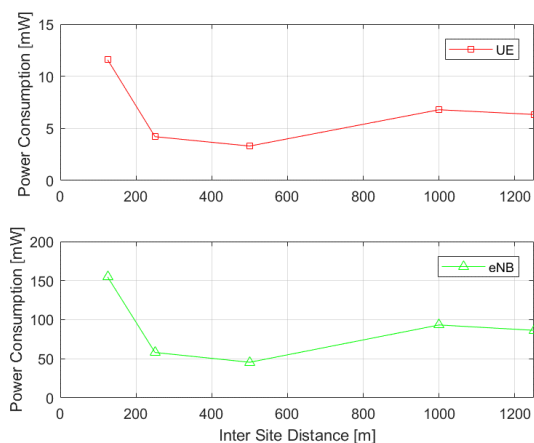


Fig. 7. Impact of ISD on average supply power consumption of the UE and eNB, for UE speed= 3km/h, offset= 1 dB and TTT= 32ms.

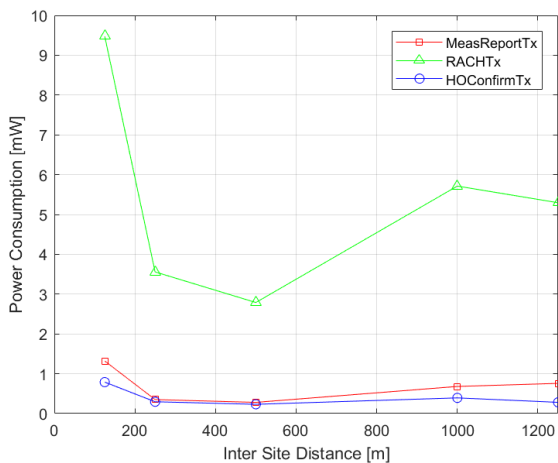


Fig. 8. Impact of ISD on average supply power consumption of various UE signaling messages transmission for speed= 3km/h, offset= 1 dB and TTT= 32ms.

V. CONCLUSIONS

A simulation analysis is presented for the signaling cost and the power consumption during HO in an LTE network when various cell size, UE speed, offset and TTT values are applied. We observe that, within the HO process, the largest contributor to air-interface signaling overhead is the

transmission of the measurement report by the UE. We note an increased signalling rate for the MeasReport transmission than for the RACH transmission, however the power consumption is higher in the latter owing to the increased number of allocated RBs. The results, and simulation setup, also depict that an optimum cell size can be found around which any increase or decrease of the cell size brings the degradation in performance in terms of increased signaling overheads and increased power consumption. This is in complete accordance with the uplink transmission limitations as noted in our previous work [6]. As expected, we assess how increasing the UE speed degrades the performance, significantly for small ISDs. By increasing the TTT and offset values, the number of HOs decreases which results in reduced signaling overheads and the power consumption, but at the cost of increased number of HO failures (as also noted in [6]). Future work will address the study of power consumption including the BBU contribution, and also accounting for the power consumption at the receivers.

REFERENCES

- [1] R. Arshad, H. Elsayy, S. Sorour, T. Y. Al-Naffouri and M. S. Alouini, “Handover Management in 5G and Beyond: A Topology Aware Skipping Approach”, *IEEE Access*, vol. 4, pp. 9073-9081, Dec 2016.
- [2] T. Bilen, B. Canberk, and K. R. Chowdhury, “Handover Management in Software-Defined Ultra-Dense 5G Networks”, *IEEE Network*, vol. 31, pp. 49-55, Aug 2017.
- [3] G. Foddiss et al., “LTE Traffic Analysis for Signalling Load and Energy Consumption Trade-Off in Mobile Networks”, *IEEE ICC*, pp. 6005-6010, 2015.
- [4] M. S. Mushtaq, S. Fowler, and A. Mellouk. “Power Saving Model for Mobile Device and Virtual Base Station in the 5G Era.” *IEEE International Conference on Communications (ICC)*, pp. 1–6, 2017.
- [5] M. Lauridsen et., “An Empirical LTE Smartphone Power Model with a View to Energy Efficiency Evolution” *Inter technology Journal*, vol. 18, pp. 172-193, 2014.
- [6] M. Tayyab, G. P. Koudouridis and X. Gelabert, “A Simulation Study on LTE Handover and the Impact of Cell Size”, *Broadnets conference*, 2018 [Accepted].
- [7] 3GPP TS 36.300, “(E-UTRA) and (E-UTRAN); Overall description; Stage 2 (Release 15)” V15.0.0, Section 10, pp. 93-143, Dec. 2017.
- [8] X. Gelabert, G. Zhou and P. Legg, “Mobility Performance and Suitability of Macro Cell Power-Off in LTE Dense Small Cell HetNets”, *IEEE 18th International Workshop on Computer Aided Modeling and Design of Communication Links and Networks (CAMAD)*, pp. 99-103, 2013.
- [9] C. Desset et al. “Flexible Power Modeling of LTE Base Stations.” *IEEE Wireless Communications and Networking Conference (WCNC)*, pp. 2858–62, 2012.
- [10] H. Holtkamp, G. Auer, V. Giannini, and H. Haas, “A Parameterized Base Station Power Model”, *IEEE Communications Letters*, vol. 17, no. 11, pp. 2033-2035, Nov 2013.
- [11] J. Rodriguez et al., “SECRET - Secure Network Coding for Reduced Energy Next Generation Mobile Small cells”, *IEEE Internet Technologies and Applications (ITA) conference*, pp. 329-333, 2017.
- [12] S. Sesia, I. Toufik, and M. Baker. “LTE--the UMTS Long Term Evolution: From Theory to Practice”, (2nd Ed.) Wiley, 2011.
- [13] 3GPP TS 36.211, “Physical channels and modulation (Release 15),” v15.1.0, Mar 2018.
- [14] 3GPP R1-091791, “Handover performance in a Manhattan scenario,” Huawei, May 2009.
- [15] 3GPP TR 36.814, “Further advancements for E-UTRA physical layer aspects (Release 9),” V9.0.0, Mar 2011.
- [16] 3GPP TS 36.331, “E-UTRA Radio Resource Control (RRC); Protocol specification (Release 9),” v9.2.0, Mar 2010.
- [17] 3GPP TS 36.133, “Requirements for support of radio resource management (Release 9),” v9.15.0, Mar 2013.